

dye, and free-electron lasers. The same method can be used to treat cases of focused-Gaussian-refractive-index media and of partially filled resonators. It can also be used when the gain or index distribution is proportional to the magnitude squared of any single Gaussian-Laguerre mode function. In future publications we will present results for these cases and extend the treatment to multiple-pass amplifiers.⁹

^(a)Permanent address: Polytechnic Institute of New York, Long Island Graduate Center, Farmingdale, N.Y. 11735.

¹H. Kogelnik, *Appl. Opt.* **4**, 1562 (1965).

²D. Cotter, D. C. Hanna, and R. Wyatt, *Appl. Phys.*

8, 333 (1975).

³W. R. Trutna, Jr., and R. L. Byer, *Appl. Opt.* **19**, 301 (1980).

⁴R. T. V. Kung, *IEEE J. Quant. Electron* **18**, 1323 (1982).

⁵H. Kogelnik and T. Li, *Appl. Opt.* **5**, 1550 (1966).

⁶B. N. Perry, R. O. Brickman, A. Stein, E. B. Treacy, and P. Rabinowitz, *Opt. Lett.* **5**, 288 (1980).

⁷The plane-wave-field gain coefficient is usually defined for Raman lasers as the exponential growth rate that would apply if the peak gain coefficient were uniform in the transverse dimension as would occur in the limit $k_g \rightarrow 0$ or $\mu \rightarrow 1$.

⁸Because the mode indices begin at zero, we have chosen the row and column indices of our matrices to begin at zero.

⁹P. Rabinowitz, A. Stein, R. Brickman, and A. Kaldor, *Opt. Lett.* **3**, 147 (1978).

Statistics of Millimeter-Wave Photons Emitted by a Rydberg-Atom Maser: An Experimental Study of Fluctuations in Single-Mode Superradiance

J. M. Raimond, P. Goy, M. Gross, C. Fabre, and S. Haroche

Laboratoire de Physique de l'École Normale Supérieure, F-75231 Paris Cédex 05, France

(Received 18 October 1982)

An experimental study of the fluctuations of a millimeter-wave transient Rydberg-atom maser is presented. The photon-number probability distribution is shown to evolve in time from a Bose-Einstein to a bell-shaped distribution. The experiment is a quantitative check of single-mode superradiance theory.

PACS numbers: 42.52.+x, 07.62.+s, 32.90.+a

Rydberg atoms, excited by a laser pulse inside a properly tuned millimeter-wave cavity, amplify the radiation noise at the cavity resonant frequency and emit a transient maser pulse.¹ By use of a very sensitive detection technique based on atomic field ionization, it is possible to actually count the atoms which have radiated during a given time interval inside the cavity, which obviously amounts to counting the number of photons emitted during that time. Such a photon-counting type of experiment is quite novel in this part of the radiation spectrum. It allows us to test under almost ideal conditions the simplest model of superradiance (the so-called "single-mode" model²). In this Letter, we present an experimental study of the pulse-to-pulse fluctuations of a Rydberg maser made of a few thousand radiators. We have observed how the histogram of the number n of emitted photons qualitatively changes during the emission time: Typical of a Bose-Einstein field at the beginning of the process, it evolves at later time into a broad bell-shaped

curve presenting a maximum peak for a value $n \neq 0$. The measured histograms have been found to be in very good agreement with the predictions of the "single-mode" superradiance theory. This is to our knowledge the first direct and quantitative test of the theory, in a system in which superradiance is not complicated—as is the case in the optical domain—by propagation or diffraction effects.³

The experimental setup is sketched in Fig. 1(a): A thermal beam of Na atoms is excited by a dye-laser pulse (5 ns duration) to the $29S_{1/2}$ level inside a millimeter-wave semiconfocal Fabry-Perot cavity tuned to resonance with the transition towards the less excited $28P_{1/2}$ level ($\nu = 162.4$ GHz). The cavity has an intermirror length $L = 1.2$ cm and a $Q = 10\,000$. It sustains a mode with a Gaussian transverse profile (waist $\omega_0 = 2.8$ mm). The small atomic sample is located at an antinode position in the mode standing-wave pattern, so that all atoms are *equivalently* coupled to the field. The atoms interaction with the cavi-

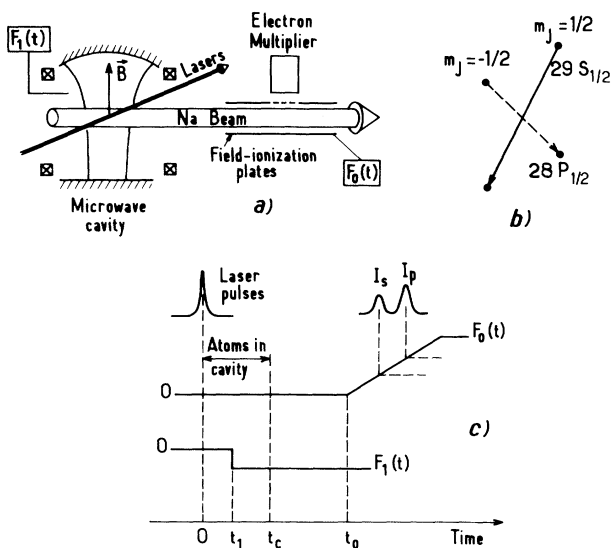


FIG. 1. (a) Sketch of the Rydberg maser setup. (b) Transition diagram showing the σ_+ and σ_- components of the masing transition in a magnetic field B , with the cavity-selected transition indicated by the solid-line arrow. (c) Sketch representing the timing of events relevant to the Rydberg maser evolution detection.

ty during a transit time $t_c \sim 2.8 \mu\text{s}$, and are detected downstream between two parallel condenser plates. The $28S_{1/2} \rightarrow 28P_{1/2}$ transition hyperfine structure plays no role in the system evolution since it is much smaller than t_c^{-1} . The masing transition is the superposition of two σ_+ and σ_- circularly polarized components corresponding respectively to $\Delta m_J = -1$ and $\Delta m_J = +1$ ($m_J = \pm \frac{1}{2}$ is the magnetic quantum number corresponding to quantization along the cavity axis). In view of a direct comparison of the experiment with theoretical models, we isolate a pure "two-level" transition in the emission process with the help of a magnetic field $B \sim 50$ G applied parallel to the cavity axis. The $\sigma_+ - \sigma_-$ degeneracy is then removed by the Zeeman effect [see Fig. 1(b)]. The cavity is tuned to resonance with the σ_+ component, so that only half of the initially pumped atoms contribute to the masing process on a *non-degenerate* transition.

The study of the system evolution is performed by applying a sequence of electric fields and by detecting the electrons resulting from atomic ionization in a high-gain electron multiplier (EM) [see timing of events in Fig. 1(c)]. A ramp of electric field $F_0(t)$ is applied between the condenser plates. It starts at a time $t_0 \sim 20 \mu\text{s}$ after the laser pulse and reaches at different times the thresholds for ionization of the $29S_{1/2}$ and $28P_{1/2}$

levels, producing two electron peaks, I_S and I_P , each being proportional to the population of the corresponding level at time t_0 . With the field $F_0(t)$ acting alone, we could probe only the *final* state of the maser evolution (since $t_0 > t_c$). In order to analyze the evolution *during* the atom-cavity interaction, a small inhomogeneous electric field $F_1(t)$ is applied inside the cavity. This field, suddenly switched on at a time $t_1 \leq t_c$, gives a Stark shift of the Rydberg levels out of resonance with the cavity mode and thus *interrupts* at this time the atom-cavity coherent coupling. The level populations then evolve from time t_1 to t_0 according to known and entirely calculable incoherent processes (spontaneous emission and transfers induced by blackbody radiation in transverse modes inside the cavity and in all field modes outside the cavity). The measurement of the atomic populations at time t_0 thus yields —after correction—the state reached by the system at time $t = t_1$. By resuming the experiment with various delays $t_1 \leq t_c$, one can sample the system evolution during the interval $t = 0$ to $t = t_c$. A LSI 11 computer analyzes the data in real time. Knowing the EM gain (with a $\pm 15\%$ uncertainty), it counts the atoms detected in I_P and I_S , corrects for the incoherent losses in the interval $t_0 - t_1$, and thus yields, for each pulse, the absolute number of masing atoms N and the partial populations $N_S(t_1)$ and $N_P(t_1)$ in the upper and lower atomic states at time t_1 . The fluctuations of these numbers have two causes: (i) N fluctuates from pulse to pulse as a result of unavoidable dye-laser instabilities. Any change in N reacts of course on N_S and N_P and also on the N_S/N_P ratio at time t_1 since the time scale of the emission depends upon the total atom number. (ii) Even for a constant N value, $N_S(t_1)$ and $N_P(t_1)$ fluctuate from pulse to pulse as a result of the quantum noise of the maser emission. As we are interested in this intrinsic noise alone, the computer selects the events corresponding to a preset N value (small $\pm 5\%$ relative acceptance). With this fixed atom number, a statistical analysis is made of 900 pulses for each t_1 and the histogram of $N_P(t_1)$ values is displayed on a graph. Clearly the $N_P(t_1)$ histogram represents also the probability $P_n(t_1)$ that n photons have been emitted up to time t_1 .

The histograms relative to $N = 3200$ atoms and corresponding—from bottom to top—to increasing times are displayed in Fig. 2. t_1 is measured in units of t_D , which is, as explained below, the "average emission delay" ($t_D = 450$ ns). At short times ($t_1 < 0.7t_D$), the histograms exhibit an expo-

nentially decreasing shape characteristic of Bose-Einstein statistics in a single radiation mode. The $P_n(t_1)$ distribution is then typical of a thermal field whose "temperature" increases with time. Around $t_1 \sim t_D$, the histograms change and start to develop into bell-shaped curves with maxima for $n \neq 0$ values, which is typical of a "coherent" emission process. Qualitatively, these results are reminiscent of similar observations in the optical domain,⁴ where the field statistics of a Q -switched laser have been studied as a function of time. In this latter case, however, the system was continuously pumped and hence evolved towards a steady state of emission. In this experiment, the atoms are instantaneously prepared at $t=0$ and emit a single burst of radiation in a process which is very closely related to the simplest model of superradiance theory.

The atomic emission into the cavity is a collective process in which all the atoms are symmetrically coupled to a damped single field mode. For very high- Q cavities, a quasiperiodic energy exchange between the atoms and the field is theoretically predicted.^{2,5} For a moderate Q , which is the case in our experiment (see exact condition below), the atoms are expected to radiate according to a monotonic irreversible process. The system evolution is then described by a master equation,⁶ which gives for the photon probability distribution $P_n(t)$

$$\begin{aligned} \dot{P}_n(t) = & -\eta_{\text{cav}}\Gamma[(N-n)(n+1)P_n - (N-n+1)nP_{n-1}] \\ & -n_B\eta_{\text{cav}}\Gamma[(N-n)(n+1)(P_n - P_{n+1}) + (N-n+1)n(P_n - P_{n-1})], \end{aligned} \quad (1)$$

where Γ is the partial spontaneous emission rate on the masing transition ($\Gamma = 43.5 \text{ s}^{-1}$ for the $29\text{S}_{1/2} - 28\text{P}_{1/2}$ line); n_B is the average number of blackbody photons per mode at frequency ν ($n_B \sim k_B T/h\nu = 38$ for $T = 300 \text{ K}$); η_{cav} is a cavity enhancement parameter describing the increase of the spectral density of modes seen by the atoms, due to the presence of the resonant cavity.⁵ η_{cav} is equal to $(\frac{3}{4}\pi^2)(Qc^3/\nu^3v)$ with $v = (\pi/4)L\omega_0^2$ being the cavity-mode effective volume (in our experiment, $\eta_{\text{cav}} = 69$). For $T = 0 \text{ K}$ ($n_B = 0$), Eq. (1) has been derived in an equivalent form in Ref. 2. The n_B -dependent terms in Eq. (1) describe the effects of thermal-field-induced transitions.⁷ Solution of Eq. (1) with the initial condition $P_n(0) = \delta_{n,0}$ (no field emitted at initial time) is given by the following analytical expression, valid for $N \gg 1 + n_B$:

$$P_n(t) = \frac{1}{1+n_B} \left(\frac{N}{N-n} \right)^2 \exp(-t/T_R) \exp\left\{ -\frac{N}{1+n_B} \frac{n}{N-n} \exp(-t/T_R) \right\}, \quad (2)$$

where $T_R = (\eta_{\text{cav}}\Gamma N)^{-1}$ is the characteristic time of the process. A formula equivalent to Eq. (2) is given by De Giorgio and Ghilmetti⁸ for $n_B = 0$. Generalization to the case where thermal photons are present is given in Ref. 6. From Eq. (2), we get the average number of emitted photons at time t : $\langle n \rangle = \sum n P_n(t)$. The time t_D corresponding to $\langle n \rangle = N/2$, called "average emission delay," is $t_D = T_R \ln[N/(1+n_B)]$. The only effect of a thermal

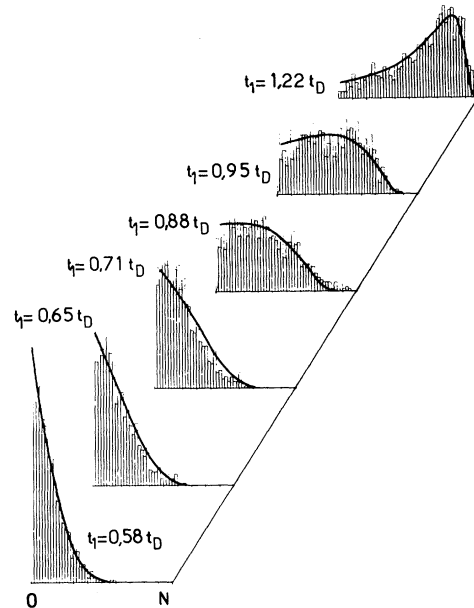


FIG. 2. $N_p(t_1)$ histograms, each corresponding to a given time t_1 , expressed in units of t_D . The histograms are constructed with 900 pulses each and they all correspond to the same value of the total atom number ($N = 3200$). The superposed solid-line curves represent the theoretical photon distributions $P_n(t_1)$, calculated from Eq. (2).

field on the system evolution is thus to translate the emission delay, without altering the nature of the photon fluctuations. This merely reflects the fact that the statistics of the vacuum field (which triggers the system if $n_B = 0$) and those of the thermal field (which start the emission if $n_B \approx 1$) obey the same Gaussian law. The condition for the regime described by Eq. (1) to occur is^{2,6}

$2\pi\nu/Q \gg T_R^{-1}$, an inequality fully satisfied in this experiment ($2\pi\nu/Q \sim 10^8 \text{ s}^{-1}$, $T_R^{-1} \sim 10^7 \text{ s}^{-1}$).

The variations versus n of $P_n(t_1)$ given by Eq. (2) have been compared with the experimental results. The best fit has been obtained for $T_R = 100(10)$ ns and $t_D = 450(50)$ ns, in good agreement with the values directly deduced from the independently measured parameters Q , n_B , ν , ν , Γ , and N [$T_R = 105(50)$ ns and $t_D = 460(200)$ ns]. The shapes of the theoretical curves (solid lines in Fig. 2) are in excellent agreement with the histograms.

This study can be considered as a precise check of the simplest model in superradiance theory and also directly demonstrates the cavity enhancement effect in spontaneous emission which was long ago predicted by Purcell.⁵ Equation (1) with $n_B = 0$ and $\eta_{\text{cav}} = 1$ has been proposed⁹ to describe the superradiance emission in free space of a small sample much smaller than $\lambda = c/\nu$ (Dicke superradiance). It has been recognized, however, that this equation is not valid in this case since it overlooks dispersive forces due to virtual exchange of off-resonant photons between closely spaced atoms.¹⁰ It has also been argued that an equation similar to Eq. (1) could be used to describe mirrorless superradiance in a large sample where the above dispersive forces are negligible. This is the so-called "mean-field" model which assumes that all the atoms see an "average" field. This assumption does overlook, however, propagation and diffraction which tend also to decrease the atomic symmetry. The only realistic system for which Eq. (1) applies thus seems to be precisely a small atomic sample inside a resonant cavity. The "single-mode" or "mean-field" assumption is then correct since all atoms "see" the same field. On the other hand, the cavity enhancement effect does speed up the symmetrical dissipative coupling of the atoms to the radiative field without appreciably increasing the dispersive forces. A last remark should be made concerning the role of temperature. Usually, superradiance theories deal with systems at $T = 0$ K whereas our experiment corresponds to $T = 300$ K ($n_B \gg 1$). In fact, it can be shown by inspection of Eq. (1) that, if $N \gg n_B$, the thermal-

field contributions become rapidly negligible because they depend upon differences ($P_n - P_{n-1}$) which tend to cancel out. Blackbody effects are relevant only at the onset of the emission, when the emitted field is still much smaller than the thermal one. At this time, however, the thermal fluctuations have the same statistical nature as the vacuum-field ones. Testing superradiance at $T = 0$ K or $T \neq 0$ K is thus basically the same experiment (provided $N \gg n_B$).

In a previous study,³ the fluctuations of the emission delay in the superradiant emission of a large sample had been measured and compared with the predictions of numerical calculation taking propagation effects into account. The novelty of our experiment is to yield not only the delay fluctuation, but also the whole photon-distribution histogram in a propagation-free situation where all the parameters of the experiment are known and the evolution of the system is described by a simply analytical expression [Eq. (2)].

¹M. Gross, P. Goy, C. Fabre, S. Haroche, and J. M. Raimond, *Phys. Rev. Lett.* **43**, 343 (1979).

²R. Bonifacio, P. Schwendimann, and F. Haake, *Phys. Rev. A* **4**, 302, 854 (1971).

³For a review of propagation effects in optical superradiant systems, see, for example, Q. H. F. Vreken and H. M. Gibbs, in *Topics in Current Physics*, edited by R. Bonifacio (Springer-Verlag, New York, 1982), and references therein.

⁴F. T. Arecchi, V. De Giorgio, and B. Quazzola, *Phys. Rev. Lett.* **19**, 1168 (1967); D. Meltzer and L. Mandel, *Phys. Rev. A* **3**, 1763 (1971).

⁵E. M. Purcell, *Phys. Rev.* **69**, 681 (1946).

⁶S. Haroche, in *Proceedings of the Les Houches Summer School, Session XXXVIII*, edited by R. Stora and G. Grynberg (North-Holland, Amsterdam, to be published).

⁷Thermal-field effects in single-mode superradiance theory have been obtained in a form equivalent to Eq. (1) by G. S. Agarwal, *Quantum Optics*, Springer Tracts in Modern Physics Vol. 70 (Springer-Verlag, New York, 1974).

⁸V. De Giorgio and F. Ghielmetti, *Phys. Rev. A* **4**, 2415 (1971).

⁹G. S. Agarwal, *Phys. Rev. A* **2**, 2038 (1970).

¹⁰F. Friedberg and S. R. Hartmann, *Phys. Rev. A* **10**, 1728 (1974).